PAPER 27

A MODEL OF THE ELECTRON CORONA WITH REFERENCE TO RADIO OBSERVATIONS*

G. NEWKIRK, JR.
High Altitude Observatory, Boulder, Colorado, U.S.A.

1. INTRODUCTION

The K-coronameter developed at the High Altitude Observatory [1] to study the electron corona outside of eclipse has been in routine use since 1956 September. Up to the present date, usable observations have been obtained on some fifty-five days, and the accumulated information on the corona out to one solar radius from the limb has permitted the development of models of the electron corona above the quiet disk, the polar regions, and the active regions. The last of these, since it departs from the spherically symmetric model, should be of interest to radio astronomers.

2. OBSERVATIONS

The basic datum from the K-coronameter consists of a tracing (Fig. 1*a*) of the quantity pB made as the instrument scans about the sun at a given distance above the solar limb. Here p is the polarization and B the radiance of the corona. Each day's tracings are calibrated by introducing known amounts of polarization into the attenuated beam from the center of the solar disk. After reducing the tracing and correcting the measures for sky polarization [2], we obtain a polar plot of pB in units of the radiance of the center of the solar disk as a function of heliocentric position angle (Fig. 1*b*). The scanning aperture for these observations is 2.4 minutes of arc in diameter. Detection of the corona to one solar radius is routine.

The average observations of pB for the period, i.e. through sunspot maximum, appear in Figs. 2, 3, and 4, along with the variation of this quantity as predicted by the van de Hulst model [3] of the corona. The van de Hulst curve has been multiplied by the appended factors to bring it into coincidence with the observed values.

3. A MODEL OF THE CORONA

The signal observed by the K-coronameter will be [3]

$$pB = B_1 - B_2 = \frac{3.44 \times 10^{-4}}{c} \int_{R_1}^{R_2} N(R)\{A(R) - B(R)\} \frac{\rho^2 dR}{R\sqrt{R^2 - \rho^2}}, \qquad (1)$$

where B_1 and B_2 are the radiances of the corona in the two perpendicular states of polarization 1 and 2 in units of 10^{-10}; $c = 1.32$ is the ratio of radiance

* This research was supported by a grant from the National Science Foundation.

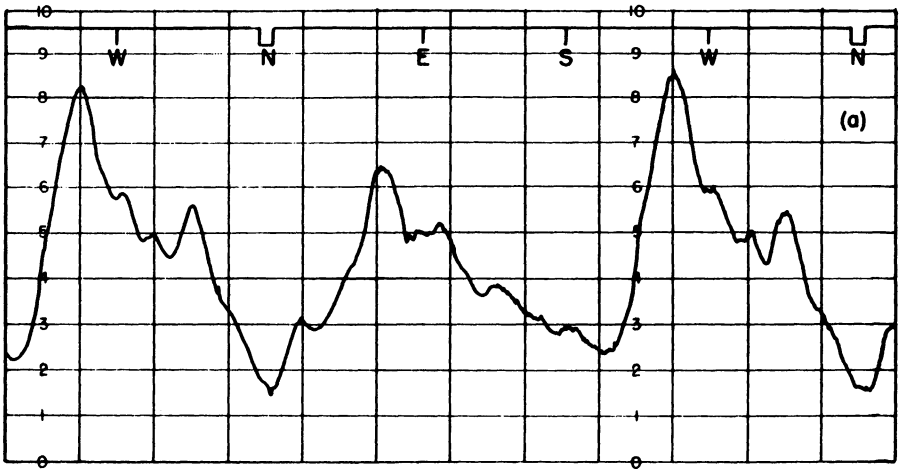

FIG. 1*a*. A tracing from the K-coronameter made as the instrument scans about the sun two minutes of arc above the limb. The north, west, south, and east position angles are marked.

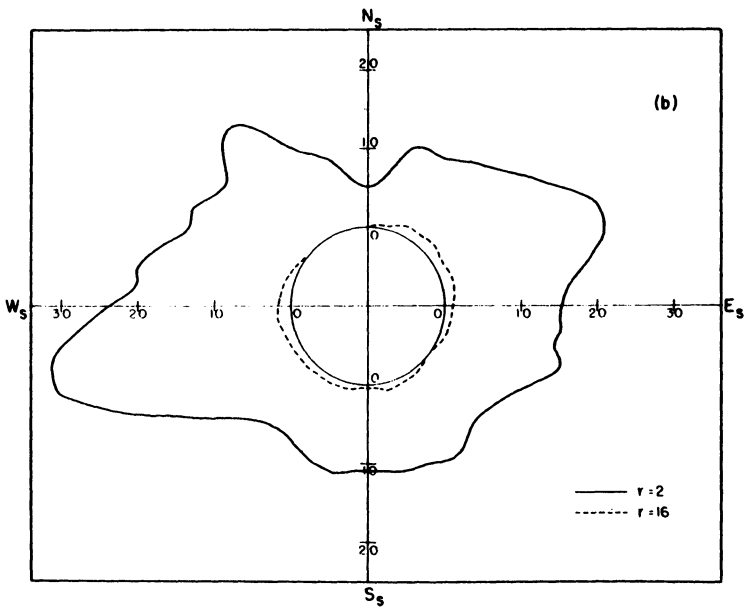

FIG. 1*b*. A polar plot of the quantity ρB as a function of heliographic position angle. Plots of the data for scan heights of 2 and 16 minutes above the limb appear. (The unit is 4.1×10^{-8} of the radiance of the center of the solar disk at 5200 Å.)

https://doi.org/10.1017/S0074180900050737 Published online by Cambridge University Press

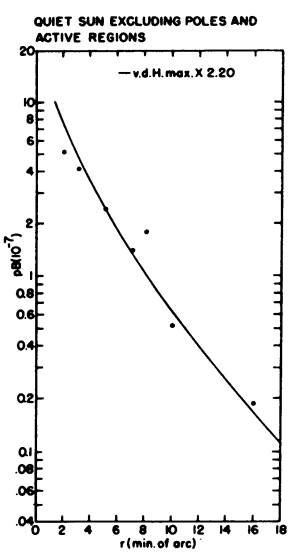

FIG. 2. Variation of pB as a function of height above the solar limb for the quiet corona.

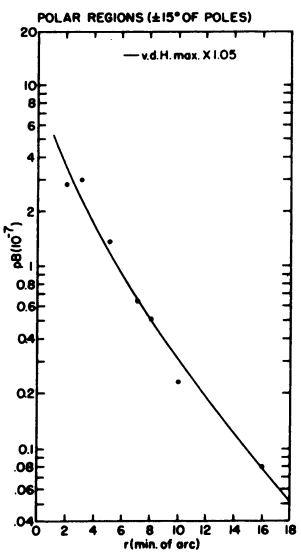

FIG. 3. Variation of pB as a function of height above the solar limb for the polar corona.

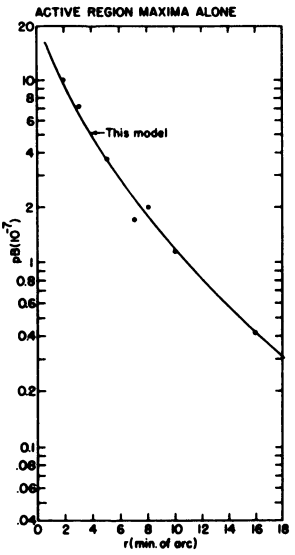

FIG. 4. Variation of pB as a function of height above the solar limb for the corona above active regions.

of the center of the solar disk to the mean radiance of the disk at 5200 Å; $N(R)$ is the electron density at distance R from the solar center (R is in units of $R_\odot$); $A(R)$ and $B(R)$ are the axes of the vibration ellipsoid for electrons at a distance R; ρ is the projected radius in units of $R_\odot$.

The usual convention is that the subscripts 1 and 2 on symbols of intensity (radiance) signify electric vectors vibrating normal to and in the plane of scattering. Equation (1) is used to determine $N(R)$ for the quiet corona and the polar regions on the basis of spherical symmetry. In this case $R_1 = \rho$, and $R_2 = \infty$. The tabulated values N_Q and N_p result (Table I).

TABLE I

R	$N_Q(10^7)$	$N_p(10^7)$	$N_a(10^7)$
1.000	90	43	73
1.125	29	14	28
1.250	12	5.7	12
1.375	5.7	2.7	5.7
1.500	3.3	1.6	2.8
1.625	2.0	.95	1.5
1.750	1.3	.62	.83
1.875	.88	.42	.48
2.000	.62	.29	.28

N_Q = electron density over quiet sun. N_p = electron density over polar regions (within 15 degrees of pole). N_a = electron density over active regions.

https://doi.org/10.1017/S0074180900050737 Published online by Cambridge University Press

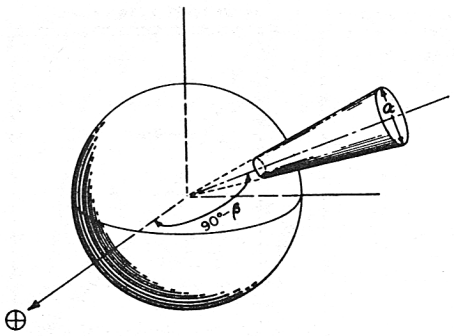

FIG. 5. Schematic diagram of the model of an active region. The enhancement of electron density is restricted to the cone of apex angle α.

The assumption of spherical symmetry is clearly invalid for the corona above active regions. The approximation used here is that the active region consists of a conical region (Fig. 5) of apex angle $\alpha = 25$ degrees containing an enhanced number of electrons $N_a(R)$ over and above the normal number. Here the integration limits are

$$R_1 = \frac{\rho}{\cos(\beta - \alpha/2)}$$
$$R_2 = \frac{\rho}{\cos(\beta + \alpha/2)} \qquad (2)$$

and equation (1) yields $2pB$. The values of the electron density $N_a(R)$ in Table 1 are found to be consistent with the K-coronameter observations. The true electron density within the confines of the cylinder is

$$N_A = N_Q + N_a \,. \qquad (3)$$

4. THE RADIO CORONA

Comparison with 21-cm observations.—An obvious test of a coronal model is to see whether or not it is able to reproduce the appearance of the sun at radio as well as at optical wavelengths. The high resolution pictures of the sun made at a wavelength of 21 cm by Christiansen and his colleagues [4] allow a direct comparison to be made. An examination of the two records (Fig. 6) shows a striking resemblance between the regions of enhanced 21-cm radiation and the regions of enhanced electron density.

Before we can perform a detailed comparison between the apparent temperature T_a and the K-coronameter signal pB at a given height, we must examine the effects of limited resolving power on both pieces of data. For this purpose it is necessary to solve the integral equation

$$S'(\rho) = \int_{-\infty}^{\infty} S(\rho) f(\rho + \rho') d\rho' \,, \qquad (4)$$

where S is the signal that would be received with infinite resolving power, S' is the observed signal, and f is the diffusion function. For the K-corona-

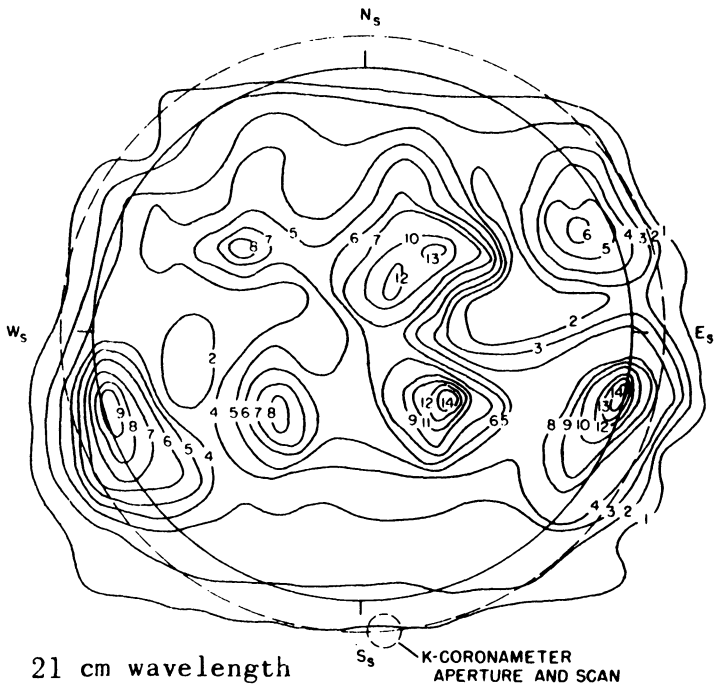

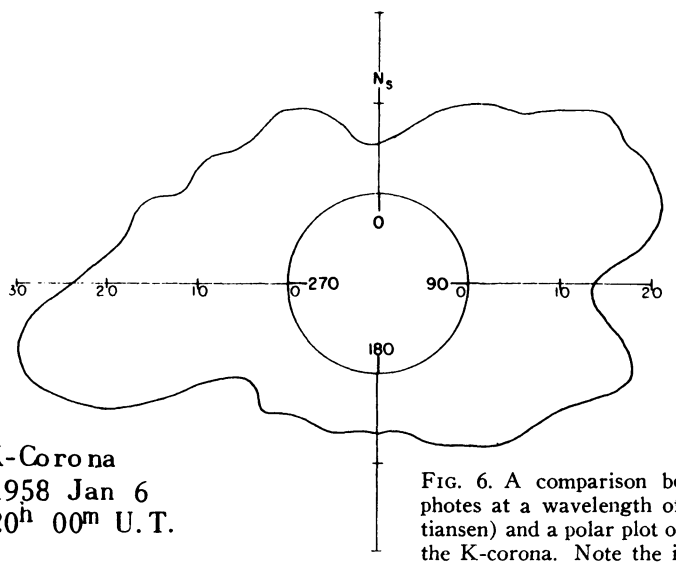

FIG. 6. A comparison between the isophotes at a wavelength of 21 cm (Christiansen) and a polar plot of the intensity of the K-corona. Note the indication of the scanning aperture and height of the K-coronameter on the radio picture.

https://doi.org/10.1017/S0074180900050737 Published online by Cambridge University Press

meter observations the diffusion function was taken as a delta function of width $2\Delta\rho'$. For the radio observations f is a gaussian of half-intensity width $2\Delta\rho'$. Solution of (4) for $S(\rho)$ by successive approximations [5] for several representative cases yields the correction factors S'/S displayed in Table II. Since the corrections to the radio data exhibit a large variation from example to example and are much smaller than the inherent scatter in the values, no correction has been applied here.

TABLE II

Type of Observation	$\Delta\rho'$ (min. of arc)	S'/S
K-corona	1.21	1.03
21-cm pencil	1.3	0.80–1.2

In Fig. 7 appear the values of T_a and pB at $\rho = 1.125$ determined from nine days when both the 32-element interferometer and the best quality K-coronameter data were available. The scatter of points is not surprising when one considers that the observations are separated by about twelve hours.

Thermal emission from active regions.—The apparent temperature at $\lambda = 21$ cm of an active region is

$$T_a = \int_0^\tau T_e(\tau)e^{-\tau}d\tau = T_e(1 - e^{-\tau}) , \tag{5}$$

where

$$\tau = \int_{x_1}^{x_2} \kappa(x)dx , \tag{6}$$

and the absorption coefficient is [6]

$$\kappa = \frac{\zeta N^2}{\nu^2 \mu T_e^{3/2}} . \tag{7}$$

Here ν = frequency of radiation, μ = refractive index, $\zeta = 0.16$, T_e = electron temperature.

Application of equation (5) to our model at $\rho = 1.125$ with $T_e = 10^6$ °K and 2×10^6 °K uniformly throughout the corona yields the two curves of T_a vs. pB displayed in Fig. 7. The general character of the observations is well reproduced by either curve.

The wavelength variation of the slowly varying component.—The regions of enhanced radio emission at 21-cm wavelength are to be identified with what has been called the *slowly varying component* on radio records of lower resolving power. We ask what wavelength variation of T_a is predicted by our model and how this variation agrees with the observations. To avoid complication, we consider T_a vs. λ for a region above the solar limb at $\rho = 1.125$. We use the expressions above but explicitly ignore the curvature of the ray trajectories. The variation of T_a with λ in an average active region for $T_e = 10^6$ °K and, in parentheses, 2×10^6 °K appears in Table III.

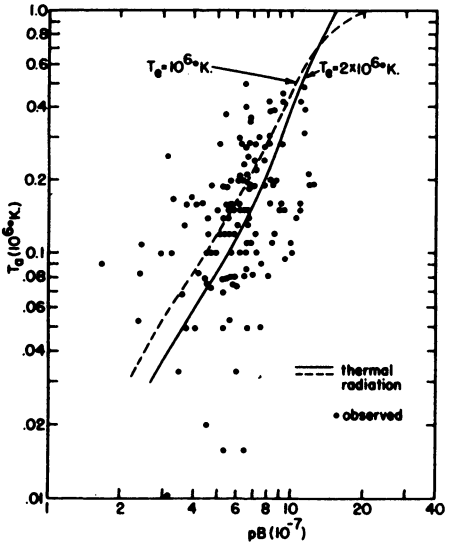

FIG. 7. The detailed relation between T_a at 21 cm and pB at a projected distance of $\rho = 1.125$ from the sun.

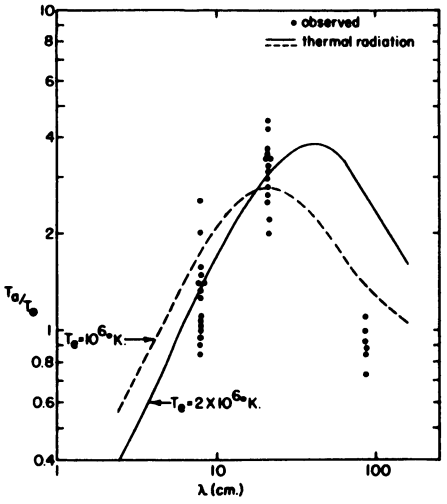

FIG. 8. The wavelength variation of T_a of the slowly varying component at $\rho = 1.125$. The unit is $T_\odot$, the apparent temperature of the center of the solar disk.

TABLE III

ν (sec^{-1})	3×10^8	10^9	1.43×10^9	3×10^9	10^{10}	3×10^{10}
λ (cm)	100	30	21	10	3	1
$T_a(10^6$°K)	1.0 (2.0)	.73 (.74)	.46 (.36)	.13 (.098)	.012 (.0091)	.0013 (.00098)
$T_\odot(10^6$°K)	.79 (.86)	.28 (.21)	.17 (.13)	.062 (.056)	.02	.008

The apparent temperature $T_\odot$ of the solar center for our corona with $T_e = 10^6$ °K and 2×10^6 °K and a chromosphere with $T_e = 3 \times 10^4$ °K [7] appears for comparison. The variation of $T_a/T_\odot$ with wavelength is shown in Fig. 8.

The comparison of this calculation with observations was made possible through the generosity of several colleagues with whom I have exchanged data covering selected dates from 1957 September through 1958 January. The pertinent information on these observations appears in Table IV. From the radio records at these wavelengths I have selected fifteen regions that were isolated knots at the solar limb in the 21-cm pictures and that would not be confused with other regions in a fan beam. To minimize errors introduced by the finite resolving power, I measured only the value of T_a at the center of the knot on the three fan-beam records. An independent determination of the undisturbed sun's signal was made by the "lower-envelope" method of Christiansen and Warburton [8], and the corresponding values of $T_a/T_\odot$ for the selected regions were plotted in Fig. 8. The agreement of the theoretical curve with the observations is satisfactory except that the data at 88 cm lie uniformly below the predicted values. Inclusion of the exact ray

trajectories in the theory would lower the calculated curve at meter wavelengths, but it remains to be seen if exact coincidence between theory and observation would result.

TABLE IV

λ (cm)	Type of Beam	Half-Power Width	Contributor	Location
7.5	fan	4.5	Kakinuma	Nagoya
21	fan	2.5	Christiansen	Sydney
21	pencil	2.5		
88	fan	4.8	Firor	Washington

5. CONCLUSIONS

In our model the region of electron density, which is double the normal electron density, is several times the diameter of the "coronal condensation" developed by Waldmeier and Müller [9]. The explanation of the regions of enhanced emission as thermal radiation at $T_e \sim 10^6$ °K is at variance with the explanation advanced by Piddington and Minnett [10] on the assumption that the source is the "coronal condensation." The major objection to the latter analysis is that the coronal condensations do not maintain the necessary high temperatures ($T_e \sim 10^7$ °K) for long periods. There is no optical evidence for regions with $T_e \sim 10^7$ °K. The small regions with temperatures up to 4×10^6 °K [11], associated with the yellow coronal line at 5694 Å, are most transitory and seldom last for more than a few hours. Undoubtedly, the yellow-line regions produce short-lived "hot spots" on the radio sun owing to their thermal emission; but they cannot be held responsible for the slowly varying component.

The active-region model used in this study is admittedly a rough approximation to the truth. A more complete model must include the conditions in the chromosphere in an active region [12] besides a smooth transition of electron density from the region's axis to the undisturbed corona. Such a sophisticated model could be used to analyze the appearance of the radio "hot spots" at positions other than the solar limb as well as to predict, after the fashion of Piddington and Minnett [10], the polarization properties of the radiation coming from such a region.

REFERENCES

[1] Wlérick, G., and Axtell, J. *Ap. J.* **126**, 253, 1957.
[2] Newkirk, G. *I.G.Y. Solar Activity Report Series* (*World Data Center A*), No. 4, 1958.
[3] van de Hulst, H. C. *B.A.N.* **11**, 135, 1950.
[4] Christiansen, W. N., *et al.* *Nature*, **180**, 944, 1957.
[5] Scarborough, J. B. *Numerical Mathematical Analysis.* Johns Hopkins Press, 1930, p. 219.
[6] Pawsey, J. L., and Bracewell, R. N. *Radio Astronomy.* Oxford, 1955, p. 83.
[7] Smerd, S. F. *Aust. J. Sci. Res. A* **3**, 34, 1950.

[8] Christiansen, W. N., and Warburton, J. A. *Aust. J. Phys.* **6**, 262, 1953.
[9] Waldmeier, M., and Müller, H. *Z. Ap.* **27**, 58, 1950.
[10] Piddington, J. H., and Minnett, H. C. *Aust. J. Sci. Res. A* **4**, 131, 1951.
[11] Billings, D. E. *Ap. J.* **125**, 817, 1957.
[12] Athay, R. G., and Thomas, R. N. *Ap. J.* **125**, 788, 1957.

Discussion

Minnaert: Are there differences between equatorial and polar electron densities?

de Jager: The problem can perhaps be solved by remembering that van de Hulst did *not* find a difference between the electron densities at pole and equator of the maximum corona. So Newkirk's results must have been compared with van de Hulst's *one* curve of N_e for the quiet maximum sun. Obviously the new result is that there now appears to be a difference in electron densities between pole and equator for the maximum sun.

Roberts: What is the factor by which the density in the active regions exceeds that in van de Hulst's model at a height about one solar radius?

Wlérick: Low in the solar atmosphere the factor is 2, and in the high corona it is 2.5.

Mathewson: We find heights of 50,000 km for our 20-cm radio sources. It is difficult to see how we obtain such heights if the electron density is only double that of the normal corona.

Wlérick: Newkirk himself recognizes that his model of an active region described by a cone of uniform density across the cross section is schematic. But, as a whole, an increase by a factor of 2 looks satisfactory.

Waldmeier: Firor's coronal model shows a region immediately over the plage area responsible for the bright radio spots on 20-cm wavelength and a second region of increased electron density high above a sunspot group that is the source for the bright radio spots on 150-cm wavelength. From optical observations of the corona one is inclined to ascribe the additional radiation on 20 cm to a *coronal condensation* of high electron density situated in the innermost part of the corona and covering the whole area of the spot group and the plage region. As the spot group dies away, a filament develops at about ten to fifteen degrees higher latitude, and in connection with it a long *coronal streamer*. At low levels the density is much larger in the condensation than in the surrounding regions, but at higher levels the maximum density is found in the streamer; therefore this may be the source for the increased radiation at 150 cm. Radio observers may check this model by verifying whether the bright radio spots on 150 cm show a higher latitude than the radio spots observed on 20 cm.

Zirin: I would agree with Professor Waldmeier that the prominence regions in the corona are associated with the slowly varying component, but I disagree that the filaments are involved. It would seem that the existence of hot loop prominences, condensing out of a dense coronal condensation, indi-

cates that the source of coronal radiation is located directly above the sunspot, where the loop prominences and coronal rain are seen.

Takakura: The temperature of the prominences is low; therefore, the brightness temperature for the radio emission at the meter wavelength radiated from the prominences cannot exceed that temperature.

Zirin: Since Newkirk's measurements were made in 1957–58, they must apply to maximum. In any event the pole-equator ratio is unimportant, since the coronal condensations occur at latitudes around 20 degrees, and the pole-equator ratio is just an accidental measure of the extent of the condensation toward the equator.